Rapid note

Roughness of sandstone fracture surfaces: Profilometry and shadow length investigations

J.M. Boffa[1], C. Allain[1,a], R. Chertcoff[2], J.P. Hulin[1], F. Plouraboué[3], and S. Roux[4]

[1] Laboratoire Fluides, Automatique et Systèmes Thermiques[b], Bâtiment 502, Campus universitaire, 91405 Orsay Cedex, France
[2] Grupo de Medios Porosos, Facultad de Ingenieria, Buenos-Aires, Argentina
[3] Institut de Mécanique des Fluides de Toulouse, avenue du Président Camille Soula, 31400 Toulouse, France
[4] Laboratoire "Surface du Verre et Interface"[c], 39 quai L. Lefranc, B.P. 135, 93303 Aubervilliers Cedex, France

Abstract. The geometrical properties of fractured sandstone surfaces were studied by measuring the length distribution of the shadows appearing under grazing illumination. Three distinct domains of variation were found: at short length scales a cut-off of self-affinity is observed due to the inter-granular rupture of sandstones, at long length scales, the number of shadows falls off very rapidly because of the non-zero illumination angle and of the finite roughness amplitude. Finally, in the intermediate domain, the shadow length distribution displays a power law decrease with an exponent related to the roughness exponent measured by mechanical profilometry. Moreover, this method is found to be more sensitive to deviations from self-affinity than usual methods.

PACS. 62.20.Mk Fatigue, brittleness, fracture, and cracks – 68.35.Bs Surface structure and topography – 42.30.Yc Other topics in imaging and optical processing

The topography of fracture surfaces has drawn a great deal of attention in recent years. As shown first by Mandelbrot *et al.* [1], these surfaces exhibit a particular scaling property known as self-affinity: statistically, they remain invariant under the transformation $(x, y, z) \to (\lambda x, \lambda y, \lambda^{\zeta} z)$. x and y are directions parallel to the mean plane of the fracture and z is the direction normal to the x, y plane. ζ is known as the roughness (or Hurst) exponent. In many cases, ζ has been found to be close to 0.8, independently of the material and of the fracture mode. Thus, it was conjectured that this value might be universal [2]. However, significantly smaller values of ζ (close to 0.5) have been reported either for inter-granular fracture as in sandstones [3] or in the case of slow propagation for metallic materials or silica glass [4,5]. These observations have been recently related to the statistical problem of pinning/depinning of a moving front in the presence of randomly distributed impurities [6,7].

Experimental investigations of fracture surfaces generally use techniques based on elevation profile recordings (measurement of z *versus* x and y). This can be achieved by direct observation of cuts perpendicular to the fracture plane or by mechanical or optical profilometry (usual profilometer or AFM depending on the length scales involved). In the present paper, we use an indirect method based on the study of the length of the shadows appearing under grazing illumination. Although optical investigations are usually very efficient, their applications to self-affine surfaces are scarce since no general relationship exists between the brightness pattern and the surface topography [8,9]. Recently, Hansen *et al.* [10] have considered the case of self-affine surfaces illuminated by a parallel light. When the angle θ between the incident beam and the mean surface plane is small, the lengths of the shadows have a broad distribution. In the trace on the surface of a cut plan parallel to the incident beam, the distribution of the shadow lengths exhibits interesting scaling properties; the number of shadows of length δ, $N(\delta)$, can be determined using an approach derived from the box-counting method [11]. First, in order to take into account the coupling between horizontal and vertical directions introduced by the oblique illumination, pavings of rectangular boxes instead of square ones are used; their aspect ratio is chosen equal to $\tan\theta$ so that a diagonal is parallel to the incident light beam. Second, as observed for many self-affine random surfaces, the height difference between two adjacent columns of the paving is assumed to follow a Gaussian distribution. Then, the number of

[a] e-mail: allain@fast.fast.u-psud.fr
[b] UMR CNRS 7608
[c] UMR CNRS/St. Gobain

shadows of length δ per unit length of profile is predicted to decrease as:

$$N(\delta) \sim (\delta/\delta_M)^{(-1-\zeta)} \quad (1)$$

where δ_M is the typical largest shadow length, which depends on the incidence angle: $\delta_M \sim (\tan\theta)^{-1/(1-\zeta)}$. Numerical simulations of the problem for ζ ranging between 0.2 and 0.8 give a good agreement with these predictions [10,11]. We apply here this method to investigate experimentally the roughness of sandstone fractures.

The sandstone samples investigated in this letter have been fractured at a very low constant velocity thanks to a precise control of the fracturation process [12,13]. Typically, the crack propagation speeds range between 3×10^{-4} m/s and 5×10^{-2} m/s. They are always lower than $10^{-4} \times v_R$ where v_R is the Rayleigh speed ($v_R \cong 10^3$ m/s). Berea sandstone is known to be a good example of homogeneous grained brittle rock. It is made of compact sand grains about 100 μm in size and is homogeneous at large scales. In our samples, the cohesion between the grains is weak so the fracture involves mainly inter-granular rupture. Thus, a cut-off in self-affinity occurs at small scales [3]. The initial sample dimensions are $7.8 \times 3.4 \times 34$ cm^3; fracturation is parallel to the largest and smallest sides and is initiated near one of the sample ends. The roughness analysis was performed on the central part of the fracture surface where the measured fracturation velocity was constant [12].

The surface roughness has first been characterized using a mechanical profilometer developed in our laboratory [3]. Elevation profiles are recorded along straight lines parallel to the mean crack propagation (x-axis). Each profile includes 2048 points with a sampling period equal to 25 μm and 20 parallel profiles spaced by 500 μm are collected. Data were analyzed using the Fast Fourier Transform method [14]; for a self-affine surface, the averaged power spectrum $P(f)$ scales as: $P(f) \sim f^{(-1-2\zeta)}$. Figure 1 displays $P(f)$ *versus* f in log-log coordinates for two samples I and II corresponding to different crack propagation velocities (I: $v = 5 \times 10^{-2}$ m/s at the high end of our experimental range of velocities; II: $v = 3.1 \times 10^{-4}$ m/s *i.e.* at the low end). The exponent found by fitting the data to a linear variation in the low frequency part of the spectrum is equal to $\zeta = 0.45$. For all the studied samples, ζ is found to be independent of the selected crack velocity and equal to $\zeta = 0.47 \pm 0.05$ [3]. This value differs from that previously measured by Plouraboué *et al.* ($\zeta \cong 0.8$) [12,13]. The discrepancy may come from the limitations of the profilometer used by Plouraboué *et al.* which scans the surface with a continuously translated probing tip; the small length scale roughness of the measured profiles may then be strongly damped and, consequently, the exponent ζ markedly overestimated. At large spatial frequencies, the curves in Figure 1 exhibit a cross-over from a self-affine behaviour at large scales to a grain dominated behaviour at small scales. For all samples, the cross-over takes place at a same spatial frequency which corresponds to the typical grain size, $l_G \cong 100$ μm [3].

Shadow length distribution measurements have been performed on the same samples. A specific experimental

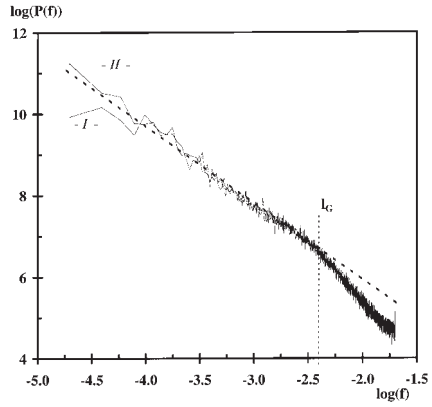

Fig. 1. Averaged power spectra computed from 20 elevation profiles of 2048 points (f is expressed in μm^{-1}). The roughness exponent found fitting the data in the low frequency part of the spectrum is equal to $\zeta \cong 0.45$. Fracture velocity is: I: 5×10^{-2} m/s; II: 3.1×10^{-4} m/s.

set-up has been built for that purpose [11]. The sample under study is installed so that the mean fracture plane is horizontal and is illuminated under grazing incidence by a parallel white beam of very small angular aperture. The beam direction is in the same vertical plane as the crack propagation direction (x) and forms an angle θ with the horizontal. The surface is observed from above using a numerical linear camera having 2048 pixels connected to a PC computer (the grey levels vary from 0 to 255). Images composed of 500 pixels $\times$ 8000 steps are recorded translating horizontally the sandstone sample with an accurate linear positioning table. The length of the image is parallel to the crack propagation direction (parallel to x). The magnification is such that one pixel corresponds to 50 μm, and the translation step size is 25 μm. Thus, images represent an area of about 2.5×20 cm^2. The very large length to width ratio, which we use, allows to reduce finite size effects on the distribution of shadow lengths. After recording, images are binarized to discriminate shadow zones from illuminated patches. This represents the most difficult stage of the experiment since usual thresholding procedures, which consist in comparing the grey level of each pixel to a prescribed constant value, lead to unreliable results. Indeed, due to light scattering and to surface self-affinity, the illumination level for a pixel inside a small shadow can be higher than that of a pixel corresponding to an illuminated zone having a small inclination with respect to the incident light. Furthermore, this effect depends on θ, the incidence angle. If θ is small, the grey levels of pixels belonging to small illuminated patches can be very low. Then, such pixels may not be identified as lightened: the corresponding illuminated patch is not detected and a long length shadow is counted instead of two smaller shadows. On the contrary, if θ is large, light scattering is very efficient and too many illuminated patches are detected. To overcome this difficulty, we have developed a local thresholding procedure and we optimize the incidence angle by comparing the experimental and the theoretical values of the total illuminated length [11]. In the experiment, the angle θ between the beam direction

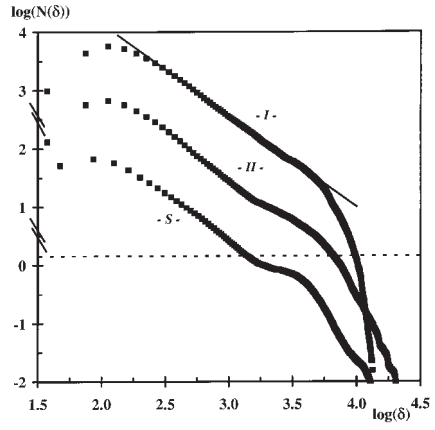

Fig. 2. Plot of the shadow number, $N(\delta)$ *versus* the shadow length, δ (in log-log scales) (δ is expressed in μm); I and II: experimental results for the same samples as in Figure 1; the incidence angle is 6.5°; for clarity, $N(\delta)$ has been divided by a factor 10 in the case of curve II. The cut-off at small length scales, δ_S, is in part related to the sand grain size l_G and the cut-off at large length scales, δ_L, to the finite illumination angle. The straight line in I corresponds to the best fit which leads to a roughness exponent in good agreement with profilometer determination. S: numerical simulation results for a synthetic self-affine profile exhibiting large scale length undulations of small amplitude and facets at small length scale; for clarity, $N(\delta)$ has been divided by a factor $10^{1.5}$.

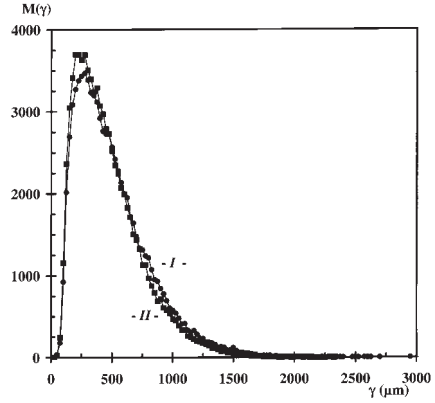

Fig. 3. Variation of the number of illuminated patches, $M(\gamma)$ *versus* patch length, γ (linear representation) (γ in μm). The experimental conditions are the same as in Figure 2, I and II.

and the fracture surface is accurately controlled by a micrometric rotation device: this is of particular importance for small incidence angles. In the following, we only report results obtained for the optimized incidence angle, which is about 5° for all the sandstone samples investigated.

Figure 2 (I and II) displays the number of shadows of length $N(\delta)$ as a function of δ in log-log coordinates for the same sandstone samples as in Figure 1. In order to reduce statistical fluctuations, each point is the mean value of $N(\delta)$ computed inside a window of size log(2) and is ascribed to the central δ value of the window. The observed curves exhibit different behaviours depending on δ which are successively considered in the following.

For small shadow lengths ($\delta \leq \delta_S \cong 100$ μm), $\log(N(\delta))$ first increases, reaches a maximum and then decreases. This complex behaviour mainly comes from the granular character of the sandstone fracture surface. A cut-off effect is indeed introduced in the geometrical properties at a length of the order of the grain size l_G: the surface is self-affine only for length scales larger than l_G. Because of the presence of the sand grain facets, there are fewer shadows of length smaller than l_G than expected for an ideal self-affine surface. It is also to be noted that the experimental determination of $N(\delta)$ is less accurate if δ is small. Indeed, at small length scales, grey level variations are more strongly influenced by light scattering; this makes difficult to identify shadows with a length of one or two pixel (*i.e.* 50 or 100 μm long) even using the local thresholding procedure we developed. This also influences the distribution $M(\gamma)$ of the illuminated patch lengths (see Fig. 3). For an ideal surface with no light scattering, Hansen *et al.* [10] expected that, due to self-affinity, the decrease of the number of illuminated patches as their size increases is very fast. Numerical simulations of the problem [11] show that, although the size distribution of the illuminated patches decreases faster than that of the shadows, it is relatively broad especially in the case of faceted surfaces such as those of sandstone samples. In agreement with our observations, the small scale cut-off of self-affinity introduced by the grain size broadens the distribution: illuminated patches of several grain sizes are observed (see Fig. 3). For all samples investigated, we find typically $M(\gamma \cong 10 l_G) \cong 0.15 M_{max} \cong 0.15 M(l_G)$ and $M(\gamma \cong 15 l_G) \cong 0.03 M_{max}$ where M_{max} is the maximum of $M(\gamma)$.

Let us now consider *large shadow lengths* ($\delta \geq \delta_L \cong 5$ mm); $\log(N(\delta))$ is observed to fall down very rapidly above $\delta_L \cong 5$ mm (see Fig. 2). The length δ_L is much smaller than the image length (20 cm); so, this decrease cannot be attributed to a finite size effect. δ_L is in fact likely to be related to the cut-off δ_M introduced by the finite angle of illumination. From the elevation profiles measured by profilometry, we can estimate the amplitude of the roughness *i.e.* the prefactor A of the power law, $\bar{\Delta} z \propto A(\bar{\Delta} x)^{\zeta}$. For samples I and II, $A \cong 10$ $\mu\text{m}^{0.55}$. δ_M is expected to verify $\delta_M \cong A^{1/(1-\zeta)} (\tan\theta)^{1/(\zeta-1)}$. In the experiments, θ equals 6.5°; a good agreement is found between the observed value $\delta_L \cong 5$ mm and the value $\delta_M \cong 4$ mm estimated in this way.

For intermediate shadow lengths ($\delta_S \leq \delta \leq \delta_L$), $\log(N(\delta))$ decreases almost linearly with $\log\delta$. In the case of sample I, the variation of $N(\delta)$ with δ can be unambiguously described by the power law variation predicted by equation (1). Fitting the experimental data leads to $\zeta = 0.55$. This value is in agreement with profilometry measurements on sample I. In the case of sample II, an unexpected bump occurs at large δ values ($\delta \cong 2$ mm). It is then difficult to determine ζ since the estimation will depend on the range of δ values used to fit the data with a power law. Varying the upper boundary of this range from 1 mm to 3 mm results in an increase of ζ from 0.40 to 0.75. The anomalously large number of shadows observed in the vicinity of $\delta \cong 2$ mm cannot be considered

as an experimental artefact. Indeed, in contrast with the case of small shadows, grey level variations are large for large shadows so that the number of such shadows is accurately determined. Furthermore, in the domain of length scales of interest, no finite size effect occurs. So, in order to explain the anomaly of the distribution around $\delta \cong 2$ mm, we have modelled the influence of defects of the fracture surface on the shadow length distribution.

In particular, we investigated the influence of smooth periodic undulations of the fracture plane having large wavelengths. For that purpose, we performed numerical simulations computing the distribution of shadows for artificial profiles: first, for ideal self-affine profiles ($\bar{\Delta}z \propto A(\bar{\Delta}x)^{\zeta}$), second for profiles modified both, at large length scales, by adding a periodic height variation ($z(x) = z_{self-affine}(x) + B\sin(2\pi x/d)$) and, at small length scales, to mimic the grain facets as previously reported [3] (practically, facet introduction does not change the results in the range of δ considered here). If no large length scale undulation is present, $\log(N(\delta))$ decreases linearly with $\log\delta$ up to the cut-off introduced by the finite angle of illumination; the measured slope corresponds exactly to the expected value: $-1-\zeta_i$ where ζ_i is the roughness exponent of the simulated profile. In the presence of an undulation (see curve S in Fig. 2), an excess of shadows is observed in the vicinity of $\delta \cong 2$ mm and the variation of $\log(N(\delta))$ with $\log\delta$ is no longer linear in spite of the very small amplitude of the applied modulation: in Figure 2, $d = 5$ mm and $B = 150$ μm (the values $\zeta = 0.45$ and $A = 10$ $\mu\text{m}^{0.55}$ were chosen to correspond to our profilometry measurements on actual sandstone samples). If we try to determine a roughness exponent, we encounter the same difficulties as for fitting data corresponding to sample II. Let us note that the contribution of such small amplitude oscillations to the Fourier spectrum power is smaller than the measurement noise. This explains why, although profilometry spectra for samples I and II are identical within the accuracy of their determination, the observed shadow length distributions are so different. This demonstrates that this distribution is very sensitive to large scale geometrical properties of the surface. On the contrary, if we consider the distribution of illuminated patches, there is no difference between numerical simulations with and without long wavelength undulations. This was to be expected since the length of illuminated patches is only governed by the small length scale cut-off (at least in the numerical simulations which do not take light scattering into account). For other sandstone samples used in the present study, the contribution of large scale undulations varies. It seems that the amplitude of the undulations increases when crack propagation velocity decreases but more experiments are needed to conclude on this point. In particular, the finite width of our samples (3.4 cm) may also influence large scale properties of the fracture surface. In the range of high crack velocities where an extended domain of linear variation is observed, the roughness exponent can be reliably determined from the variation of $\log(N(\delta))$ with $\log\delta$; its value is then always found to be in agreement with profilometry measurements.

In conclusion, we have demonstrated some of the possibilities offered by measurements of shadow length distributions on self-affine surfaces illuminated under grazing incidence. Experimental length distribution of shadows and illuminated patches measured on sandstone fracture surfaces are well described by taking account respectively the effects of surface facets and of light scattering at small length scales ($\delta \leq \delta_S$), and the finite illumination angle at large length scales ($\delta \geq \delta_L$). In the intermediate domain of δ values ($\delta_S \leq \delta \leq \delta_L$) where a power law variation is expected for $N(\delta)$, we find that the shadow length distribution is very sensitive to small amplitude deviations from self-affinity (such as undulations for instance). In the absence of surface defects, the roughness exponent deduced from shadow length distribution agrees with the value expected from profilometry measurements. The shape of the distribution also provides quantitative data on the amplitude of the rugosity. The analysis of the dependence of the distribution on the illumination angle may finally give qualitative indications on the surface defects. This method thus appears to complement well profilometry. Furthermore, complementary studies on different types of materials are under way in order to determine the range of the validity and applications of this new method.

The fractured Berea sandstone samples used in the present work have been realized at the Schlumberger Ridgefield Research Center (F. Plouraboué, K. Winkler). We are grateful to G. Chauvin and C. Saurine for their contribution to the realization of the experimental setup. Laboratoire "Fluides, Automatique et Systèmes Thermiques" is a laboratory of Paris VI, Paris XI and CNRS (UMR 7608). We thank the ARC "Géothermie des Roches Sèches" of the ECODEV program and the PNRN program. This work is part of the thesis of J.M. Boffa sponsored by the "Ministère de l'Enseignement Supérieur et de la Recherche".

References

1. B.B. Mandelbrot, D.E. Passoja, A.J. Paullay, Nature **308**, 721 (1984).
2. see E. Bouchaud, J. Phys.-Cond. **9**, 4319 (1997) and references therein.
3. J.M. Boffa, C. Allain, J.P. Hulin, Eur. Phys. J. AP **2**, 281 (1998).
4. V.Y. Milman, R. Blumenfeld, N.A. Stelmashenko, R.C. Ball, Phys. Rev. Lett. **71**, 204 (1993).
5. E. Bouchaud, S. Navéos, J. Phys. I France **5**, 547 (1995).
6. J. Schmittbuhl, S. Roux, J.P. Vilotte, K.J. Maloy, Phys. Rev. Lett. **74**, 1787 (1995).
7. P. Daguier, B. Nghiem, E. Bouchaud, F. Creuzet, Phys. Rev. Lett. **78**, 1062 (1997).
8. J.C. Russ, *Fractal Surfaces* (Plenum Press, New York, 1994).
9. J.C. Russ, J. Comput. Assist. Microsc. **5**, 171 (1993).
10. A. Hansen, F. Plouraboué, S. Roux, Fractals **3**, 91 (1995).
11. J.M. Boffa *et al.* (to be published).
12. F. Plouraboué, K.W. Winkler, L. Petitjean, J.P. Hulin, S. Roux, Phys. Rev. E **53**, 277 (1996).
13. F. Plouraboué, Ph.D. thesis, University Paris-VII (1996).
14. J. Schmittbuhl, J.P. Vilotte, S. Roux, Phys. Rev. E **51**, 131 (1995).